ANALYSIS OF SUBMERGED SMALL PUNCH TEST UNDER STATIC LOAD FOR ITS EMPLOYEMENT IN HYDROGEN EMBRITTLEMENT SITUATIONS ON HIGH AND MEDIUM STRENGTH STEELS

B. Arroyo[1*], J.A. Álvarez[1], F. Gutiérrez-Solana[1]

[1] LADICIM (Laboratorio de la División de Ciencia e Ingeniería de los Materiales), Universidad de Cantabria. ETS Ingenieros de Caminos, Canales y Puertos, Av/Los Castros 44, 39005, Santander, España
* Persona de contacto: arroyob@unican.es

RESUMEN

En este trabajo se analizan dos aceros de media y alta resistencia bajo escenarios de fragilización por hidrógeno, mediante el empleo de ensayos Small Punch (SPT) sumergidos bajo carga estática sobre probetas pre-cargadas en hidrógeno.

Se llevan a cabo ensayos de tracción a baja velocidad (SSRT) normalizados, y los ensayos SPT anteriormente citados. Se comprueba para estos escenarios una propiedad indicada en el código de buena práctica más orientada a fluencia, que indica que el valor de la velocidad de deformación en un ensayo SSRT y de desplazamiento de punzón en un SPT tienen valores numéricos semejantes cuando el tiempo de rotura en ambas situaciones es similar. Finalmente se proponen metodologías para determinar las velocidades de propagación en ambiente agresivo mediante el empleo de ensayos SPT.

PALABRAS CLAVE: Ensayo Small Punch bajo carga estática; Fragilización por hidrógeno;

ABSTRACT

In this work two steels, of medium and high strength, are analyzed under hydrogen embrittlement scenarios using submerged Small Punch tests (SPT) under static load, on specimens pre-charged in hydrogen.

Standard slow strain rate tests (SSRT), and the aforementioned SPT tests are performed. For these scenarios, it was checked a property proposed in the code of practice, mainly focused on SPT creep tests. It indicates that the deformation rate in a SSRT and punch displacement in an SPT have similar numerical values when the breaking times in both tests are alike. Finally, practical methodologies are proposed to determine propagation rates in an aggressive environment using SPT tests.

KEYWORDS: Small Punch test under static load; Hydrogen embrittlement

1. INTRODUCTION

The effect of hydrogen is especially significant in high-strength steels exposed to aqueous environments under cathodic protection (such as off-shore platforms) [1] or those typical of H_2S presence (as in gas transport pipelines). There are particular situations where standards cannot be followed to perform characterizations on in-service components, mostly due to the impossibility of machining specimens fitting the dimensions, or mainly the thickness required. One of those situations is usually present in the welded joints. To find a solution for these types of scenarios, the Small Punch Test is one of the most notables alternative tests employed. It is based on punching a reduced dimension plane specimen, which allows parameters such as the yield stress, ultimate tensile strength and even fracture toughness of metallic materials to be estimated with high reliability [2]. Over the last years some authors have proved the validity of the SPT when used in HE and SCC characterization [2÷7], having the advantage of being faster and easier than standard tests. The main objectives of this work are:

- To propose an experimental methodology to perform characterizations in hydrogen embrittlement scenarios using the small punch test under static load.
- To provide an interpretation of the measures obtained from the test (punch displacement vs. time), comparing them to those defined by standardized procedures during SSRT tests.

2. MATERIALS AND CONSIDERATIONS

2.1. Materials

For this work two materials were used: a Cr-Ni-Mn high-strength steel, which is employed in the manufacture of large anchor chain links for off-shore platforms, was used as a reference material for the studies; and a Cr-Ni mid-strength steel, widely used in the fabrication of industrial transmission shafts, was added in order to enrich the experimental results. their main mechanical properties were obtained, which are shown in Table 1. Their microstructures, presented in Figure 1, are tempered martensite in both cases.

Table 1. Cr-Ni-Mn steel mechanical properties in air.

PARAMETER		Cr-Ni-Mn	Cr-Ni
Yield Stress (MPa)		920	509
Ultimate Stress (MPa)		1015	708
Young's Modulus (GPa)		205	210
Ramber-Osgood Parameters	n	14,5	--
	α	1,15	--
$J_{0,2}$ (KN/m)		821	--
$K_{J0,2}$ (MPa*$m^{1/2}$)		410	--
Hardness (HBW30)		352	200

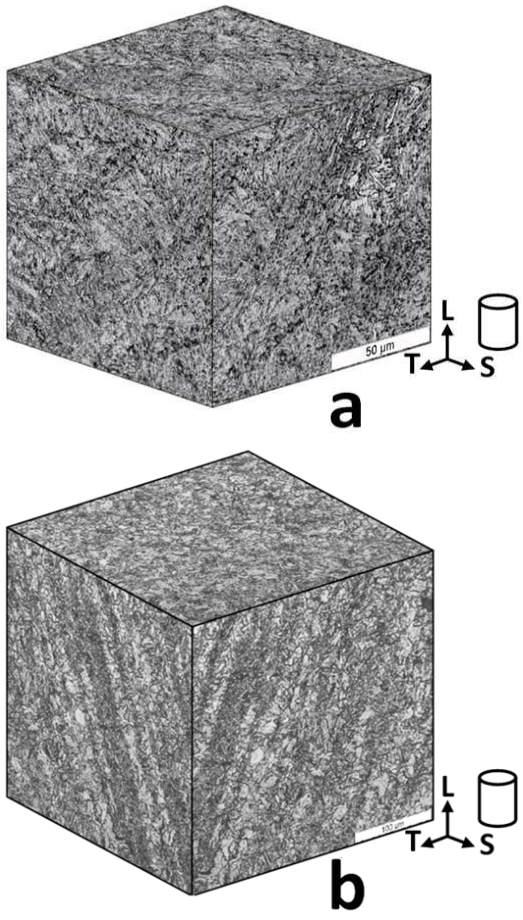

Figure 1. Microstructures of the steels used in this work. a) Cr-Ni-Mn; b) Cr-Ni.

2.2. Simulating hydrogen embrittlement

An environmental condition known as cathodic charge, or anodic polarization, has been employed in this study. It is used to protect against corrosion structures that operate in aggressive environments, or to reproduce local situations where a huge amount of hydrogen is present. It causes substantial embrittlement on the steel by the action of the hydrogen going through and getting trapped in it. Figure 2 shows a set-up of the method used in this work. It consists of the interconnection, via an acid electrolyte, of a noble material (platinum in this case) and the steel, which will protected due to the fixed current interposed [8]. In this study, for the cathodic charge situations, an environmental condition in accordance with [4,7,9] was proposed, consisting of an 1N H_2SO_4 solution in distilled water containing 10 drops of CS_2 and 10mg of As_2O_3 dissolved per liter of dissolution. The solution of As_2O_3 was prepared using Pessouyre's method. A platinum grid was used as an anode. The PH was controlled in the range 0,65 - 0,80 during the tests and at room temperature 20ºC - 25ºC. Two embrittlement levels of 5mA/cm^2 and 1mA/cm^2 were employed in this work.

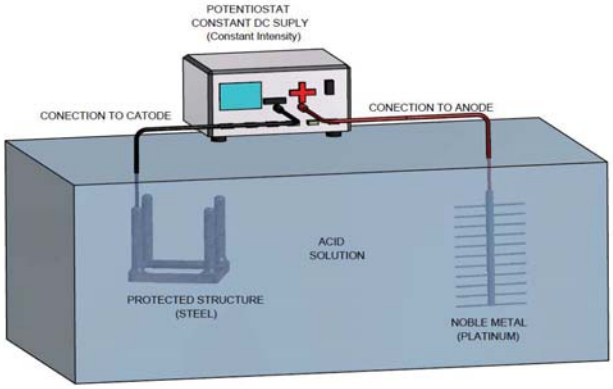

Figure 2. Schematic of the cathodic charge method.

2.3. The Small Punch test

The SPT can test in-service structures [10,11,12], since the extraction of a sample with such a small amount of material required for the Small Punch Test does not compromise the integrity of the component. It has been successfully employed in the evaluation of the tensile [10,13] and fracture [10,14] properties of different materials. Over the last few years, many groups have developed creep behavior models [15,16]. This technique has been applied to characterize embrittlement processes in steels, such as the evolution of material properties with neutron or proton irradiation [17], the brittle-ductile transition temperature of metallic materials [18], stress corrosion cracking scenarios [2], or, more recently, environmental embrittlement [3÷7]. The Small Punch Test consists of punching a plane specimen of small dimensions and deforming it until fracture. The typical shape of the registers obtained from SPT tests is presented in Figure 3.

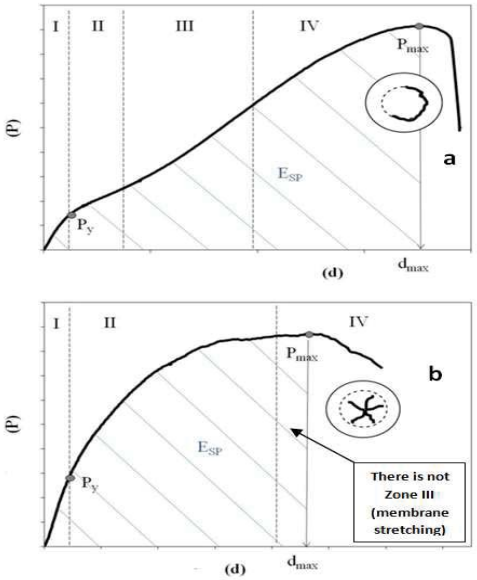

Figure 3. Typical SPT curves. Extracted from [10]; a) Ductile materials; b) Brittle behaviour.

A schematic of the device and samples used for the performance of these tests is represented in Figure 4.

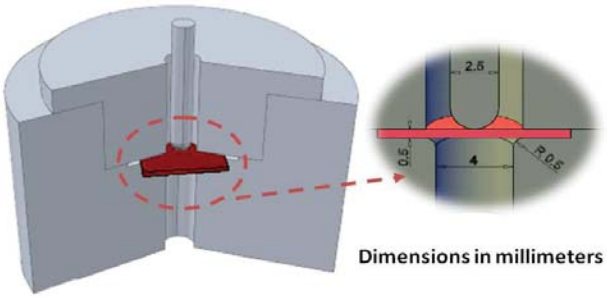

Figure 4. Schematic of SPT device and samples.

2.4. SPT considerations in aggressive environment

Standards for conventional environmental characterizations [19] require the tests to be performed at very low (quasi static) solicitation rates, while the specimen is totally submerged. This ensures a steady state of hydrogen embrittlement [9,20].

The latest research shows that the small punch test is a useful tool when applied to the estimation of steel properties in hydrogen embrittlement and stress corrosion cracking scenarios. However, SPT estimations could be conservative [3] due to the punch rate conventionally used [11], that in the most aggressive environments is too high to allow the hydrogen damaging capability to act completely in the new surfaces of the crack tip in generation. In order to obtain more accurate results, it would be useful to reproduce the same micromechanisms that take place during fracture mechanics tests. To fulfill this recommendation, recent publications have pointed to the advantages of performing the SPT at a very low constant rate or static load tests [2] while submerging the specimen during the whole process [4÷7].

3. EXPERIMENTAL METHODOLOGY

3.1. SPT experimental methodology

In a cathodic charge environment, seven Cr-Ni-Mn and four Cr-Ni SPT specimens, obtained from the straight zones of a Ø120mm chain link and Ø25mm shaft, were tested. The specimens were machined in accordance with [10,11], in an orientation such that the plane faces were transversal to the longitudinal axes of the components (cylindrical). Their specific dimensions were 10mmx10mm of section and 0.5±0.01mm of thickness (Figure 3). The test plan carried out is presented in Table 2.

Table 2. SPT test plan

MATERIAL, ENVIRONMENT AND LOAD (N)			SAMPLES TESTED	RESSULT
Cr-Ni-Mn	5 mA/cm^2	883	1 SPT	**tr**; Vsp
		667	1 SPT	**tr**; Vsp
		608	1 SPT	**tr**; Vsp
		583	1 SPT	**tr**; Vsp
		534	1 SPT	**tr**; Vsp
		509	1 SPT	**tr**; Vsp
		461	1 SPT	**tr**; Vsp
Cr-Ni	1 mA/cm^2	782	1 SPT	**tr**; Vsp
		502	1 SPT	**tr**; Vsp
	5 mA/cm^2	953	1 SPT	**tr**; Vsp
		782	1 SPT	**tr**; Vsp

Prior to the test, the specimens were subjected to hydrogen charging by exposing them for 2 hours to the corresponding environment, a period of time considered sufficient for a proper and complete diffusion of the hydrogen inside the material [9]. Subsequently, the load was softly applied by an endless screw system on the specimen subjected to the environment. The test was considered over when the sample failure occurred, thus allowing both the time up to failure (tr) and the punch rate (Vsp) to be obtained. For the purpose of this test, an experimental device was designed and built, as presented in Figure 5.

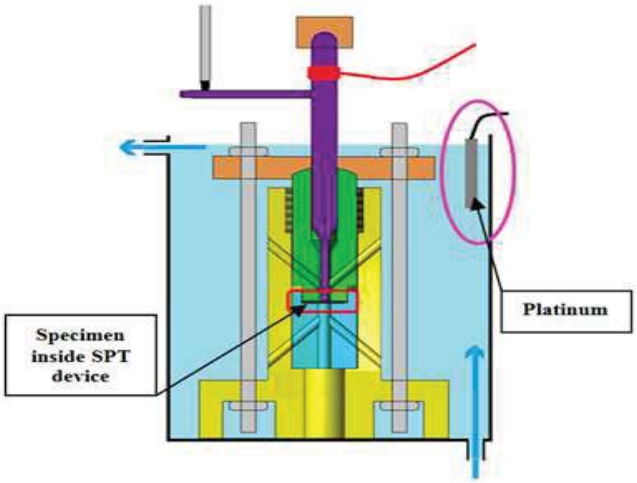

Figure 5. Schematic of SPT static load device.

4.2. SSRT experimental methodology

The study indicated the need to analyze the loading rate in each case [9,7]; hence two quasi-static loading rates were applied in accordance with [19]. From the straight zone of a Ø120mm chain link of the Cr-Ni-Mn steel, four tensile specimens of Ø9mm were obtained in accordance with [11,19]. The specimens were machined parallel to the longitudinal axis of the chain link. The result of all this was the SSRT test plan shown in Table 3. SSRT tests were not performed on the Cr-Ni steel.

Table 3. SSRT test plan

	RATE	RESSULT
Cr-Ni-Mn	6.10^{-8}m/s	$\sigma_{Max-EAC}$; $\sigma_{Med-EAC}$; t_r; $d\varepsilon/dt$
	6.10^{-9}m/s	$\sigma_{Max-EAC}$; $\sigma_{Med-EAC}$; t_r; $d\varepsilon/dt$
	6.10^{-8}m/s	$\sigma_{Max-EAC}$; $\sigma_{Med-EAC}$; t_r; $d\varepsilon/dt$
	6.10^{-9}m/s	$\sigma_{Max-EAC}$; $\sigma_{Med-EAC}$; t_r; $d\varepsilon/dt$

A stress concentrator was introduced in the central part of the shank, in order to focus the failure on that part, as shown in the schematic of Figure 6a. A finite element simulation was carried out in order to obtain the stress concentration factor at the thinnest point (Figure 6b), the value obtained being 3.93; this value was compared to the one given by [22], which was 4.09. A mean value of 4.00 was employed for further analysis.

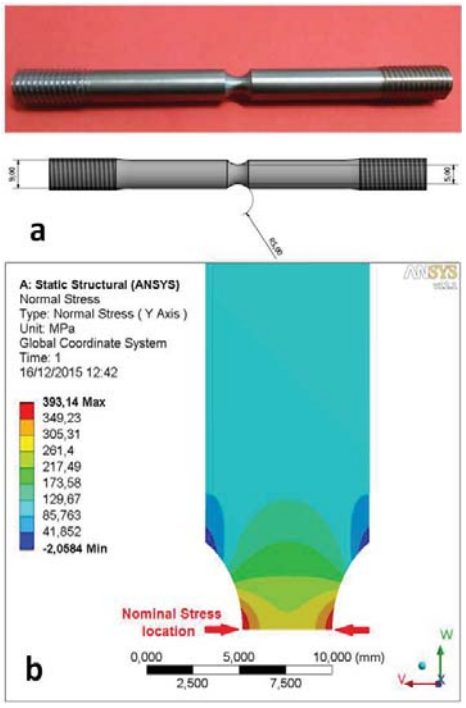

Figure 6. a) Schematic of SSRT specimens. b) Finite element analysis of the stress concentration factor.

Prior to the test, the specimens were subjected to hydrogen absorption by exposing them for 48 hours to the same environment and aggressiveness conditions as the test itself, a time considered sufficient [9] for a proper hydrogen diffusion. The test was performed subsequently by applying the corresponding loading rate using a slow strain rate machine, in accordance with the Standard ISO-7539 [19].

An analysis was carried out by obtaining the peak (maximum) and the nominal (medium) breaking stresses, $\sigma_{Max-EAC}$ and $\sigma_{Med-EAC}$, the time to rupture, t_r, and deformation rate of the necked zone, $d\varepsilon/dt$, from each test, employing for this purpose the methodology based on the ISO-7395 procedure [19].

4. RESSULTS AND DISCUSSION

4.1. SPT experimental ressults

Figure 7 presents the curves registered from the SPT tests carried out on the Cr-Ni-Mn steel. The shape of the curves clearly resembles those obtained from creep tests. In these curves three zones can be distinguished: The first one, of indentation on the and load settlement combined with crack incubation, in which an important punch displacement takes places in a short time; the second zone, after the first turning, at which a quasi-constant punch rate takes place while cracks grow; the third zone, after the second turning, in which the cracks have grown to such an extent that the rupture of the specimen becomes imminent, causing again an important punch displacement in a short time and the total drilling of the specimen. The second part, as happens in creep scenarios [16], is the most representative and could be characterized by a steady displacement rate V_{sp}, in this work it is calculated by a linear fit of punch displacement and time.

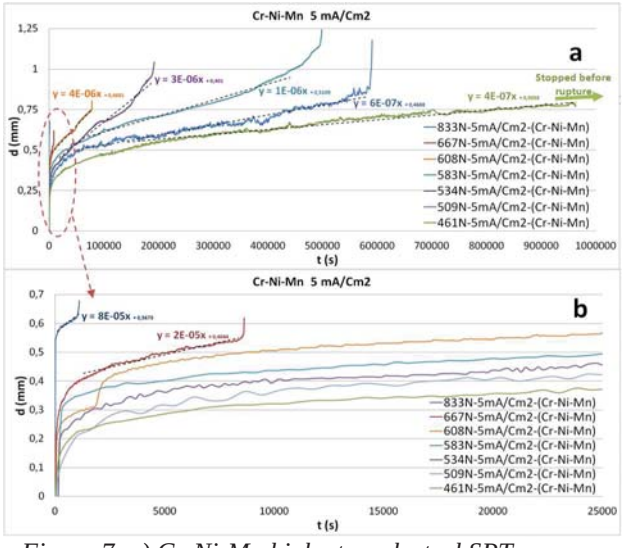

Figure 7. a) Cr-Ni-Mn high-strengh steel SPT curves under 5 mA/cm^2 environment performed. b) Zoom of those curves with lowest times to rupture.

Fractographic images were obtained. For the Cr-Ni-Mn steel, Figure 8a shows a mainly brittle transgranular fracture [1,9], present in all its test excepting the one under 461 N, which was stopped after 278 hours had elapsed (almost 12 days) and is presented in Figure 8b.

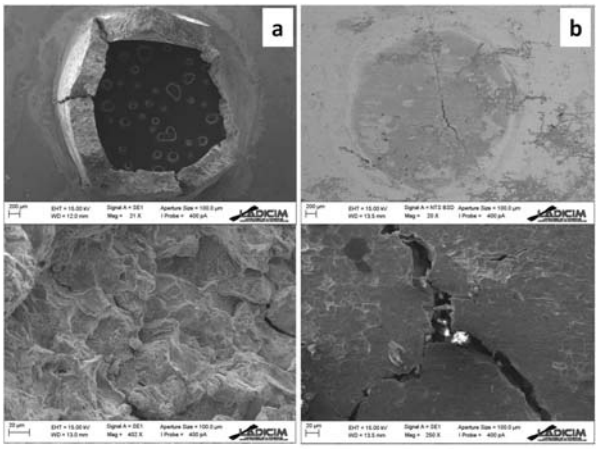

Figure 8. Fractographies of Cr-Ni-Mn under static SPT tests. a) Test under 667 N. b) Test under 461N.

In Figure 9 the whole set of results obtained is presented. For each test, the time to rupture versus the force applied is represented, showing how the lower the force applied, the higher the time to rupture. The trend described has been plotted using an exponential fit.

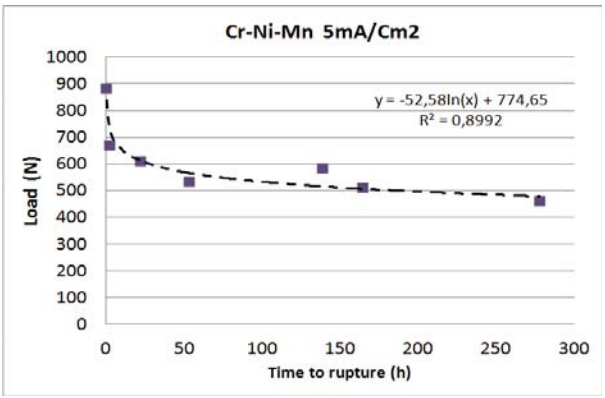

Figure 9. Representation of the load applied versus time to rupture under static SPT tests.

This behavior is present in other type of tests where the environment governs the behavior, such as standard stress corrosion cracking tests, or creep tests, both conventional or small punch creep tests [16]. In these scenarios, the time to rupture increases when the effort applied is progressively decreased, up to a threshold effort at which the time to rupture tends to infinity, so that for lower values the failure does not take place. Regarding this, it can be stated that the Small Punch test is a tool which can be used to predict a parameter of failure in embrittlement scenarios, such as the threshold SPT load, or to estimate the threshold stress in the material.

Figure 10 presents the curves registered from the SPT tests carried out on the Cr-Ni steel, obtaining similar results to the ones presented for Cr-Ni-Mn steel. On Figure 11, fractographic images from both tests under 782N in a 5 mA/cm^2 and 1 mA/cm^2 environments are presented, showing brittle scenarios [3,10], which were also observed in the other two samples tested.

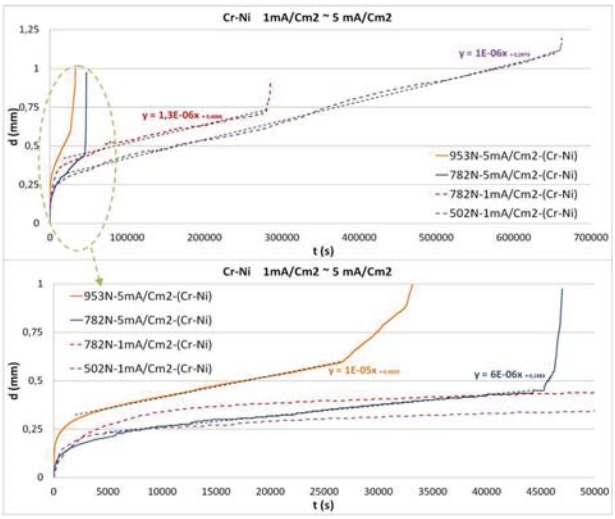

Figure 10. a) Cr-Ni mid-strength steel SPT curves under 1 and 5 mA/cm^2 environments performed. b) Zoom of the curves having the lowest times to rupture.

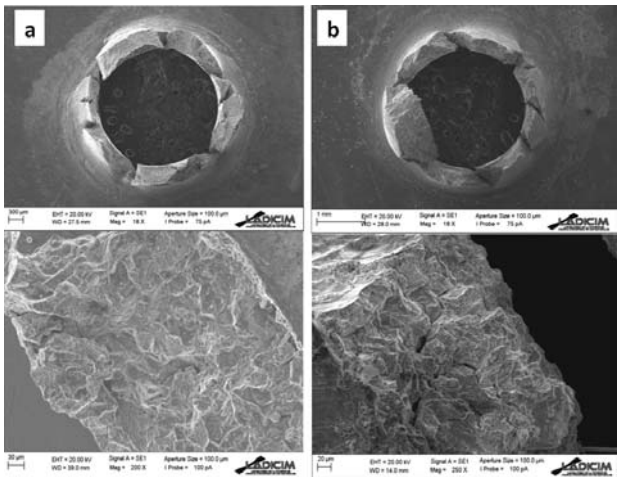

Figure 11. Fractographies of Cr-Ni-Mn under 782 N static SPT tests. a) 5mA/cm^2; b) 1mA/cm.

Below, in Table 4, the results of the whole SPT experimental campaign are summarized. For each test, the time to rupture, t_r, and the punch rate in the quasi-constant zone, V_{sp}, are indicated.

Table 4. Results obtained from SPT tests.

MATERIAL, ENVIRONMENT AND LOAD (N)			SAMPLES TESTED	RESSULT
Cr-Ni-Mn	5 mA/cm^2	883	1 SPT	**tr**; Vsp
		667	1 SPT	**tr**; Vsp
		608	1 SPT	**tr**; Vsp
		583	1 SPT	**tr**; Vsp
		534	1 SPT	**tr**; Vsp
		509	1 SPT	**tr**; Vsp
		461	1 SPT	**tr**; Vsp
Cr-Ni	1 mA/cm^2	782	1 SPT	**tr**; Vsp
		502	1 SPT	**tr**; Vsp
	5 mA/cm^2	953	1 SPT	**tr**; Vsp
		782	1 SPT	**tr**; Vsp

4.2. SPT experimental ressults

In Table 5, the results of the SSRT experimental campaign are summarized. Two different concepts are used for each case: the average rupture stress in the section, $\sigma_{Med-EAC}$, and the maximum one, $\sigma_{Max-EAC}$. In some cases, $\sigma_{Max-EAC}$ (1 mA/cm^2 environments) turned out to be higher than the yield stress, showing that there was partial plastification in the section.

Table 5. Results obtained from SSRT tests.

CONDITIONS		$\sigma_{Max\ EAC}$ (MPa)	$\sigma_{Med-EAC}$ (MPa)	tr (h)	dε/dt (1/s)
1 mA/cm^2	6.10^{-8}m/s	1485	**1224**$^{(*)}$	**16.34**	**8.56 · 10^{-6}**
	6.10^{-9}m/s	1127	**929**	**132.93**	**1.77 · 10^{-6}**
5 mA/cm^2	6.10^{-8}m/s	711	**586**	**11.93**	**9.36 · 10^{-6}**
	6.10^{-9}m/s	450	**371**	**82.93**	**1.57 · 10^{-6}**

Figure 12 shows a fracture SEM image of a specimen tested in the most aggressive environment (5mA/cm^2 at 6.10^{-9}m/s). It can be observed how a quasi brittle fracture, showing intergranular zones with some cleavage in which an important tearing present. This is a similar micromechanism as the one found on the SPT tests performed in both steels.

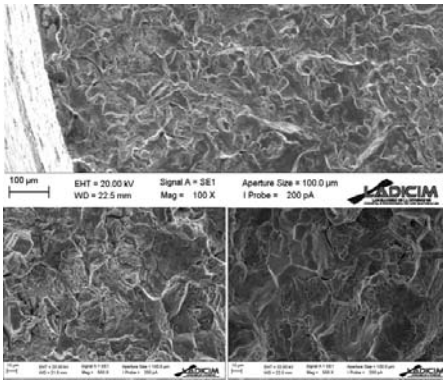

Figure 12. General fractography and details of the SSRT performed under 5mA/cm^2 and 6.10^{-9}m/s, the most aggressive environment.

5. ANALYSIS OF RESSULTS

Figure 13 shows the results of the SSRT performed on the Cr-Ni-Mn steel in the two environments and two loading rates for each one. It presents a representation of both stresses, average rupture stress $\sigma_{Med-EAC}$ and maximum one $\sigma_{Max-EAC}$, versus time to rupture. It can be observed in both environments, and for both stresses, how the stress and time to rupture have a logarithmic trend for a given combination of material and environment. Below, in Figure 14, the static load SPT tests are presented for the materials studied in terms of load applied versus time to rupture. As previously presented in Figure 9 for the Cr-Ni-Mn steel, it can be observed how, for a given combination of material and environment, a logarithmic trend is evident between the static load applied on a SPT specimen and its time to rupture. It can be also observed the influence of the environment on the Cr-Ni steel behaviour.

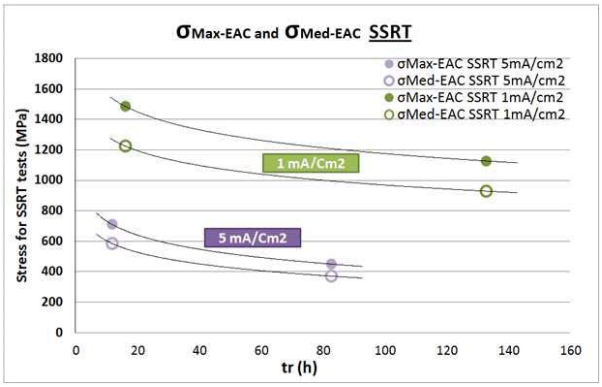

Figure 13. Cr-Ni-Mn high-strength steel representation of the average rupture stress, $\sigma_{Med-EAC}$, and maximum one, $\sigma_{Max-EAC}$, versus time to rupture under SSRT tests in the 5mA/cm^2 and 1mA/cm^2 environments.

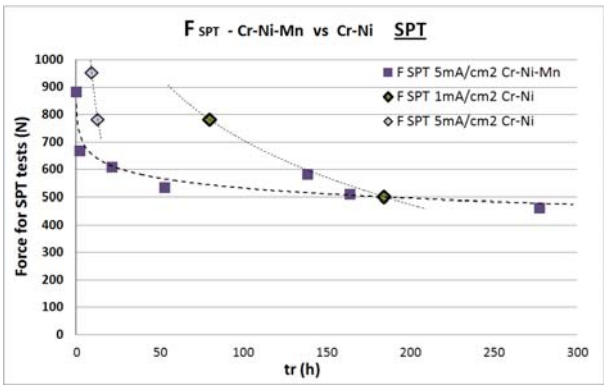

Figure 14. Cr-Ni-Mn and Cr-Ni steel representation of the force applied versus time to rupture under static SPT tests in the environments studied.

From previous results it can be stated that, for a given material in a certain environment, both the logarithm trends between stress and time to rupture for SSRT tests, and the load versus time to rupture for SPT tests can be defined, as presented in Figure 15.

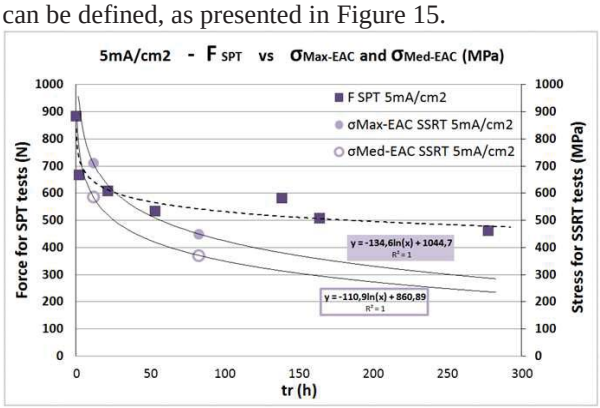

Figure 15. Comparison of SSRT and SPT tests under the 5mA/cm^2 environment. Representation of $\sigma_{Med-EAC}$ and $\sigma_{Max-EAC}$ versus time to rupture under SSRT tests, and force versus time to rupture for SPT tests.

In this context, as is usually done in SPT creep scenarios [16], a relationship between the load of the SPT tests (F) and the stress of the uniaxial tests ($\sigma_{Max-EAC}$) under the same environment can be established for similar times to rupture, a condition used to ensure the equivalence of the two tests [11, 16]. Expressions of the type (1) can be proposed to adjust a correlation between SPT test forces and SSRT stresses.

$$\frac{F}{\sigma_{Med-EAC}} = f(K_{Med}) \quad ; \quad \frac{F}{\sigma_{Max-EAC}} = f(K_{Max}) \qquad (1)$$

Where $\sigma_{Med-EAC}$ and $\sigma_{Max-EAC}$ are the average and maximum SSRT stresses, F is the force applied during an static SPT test, K_{Med} and K_{Max} are the regression coefficients.

In Figure 16, for the Cr-Ni-Mn steel under 5mA/cm^2, trends between the force in SPT static load tests and the average and maximum stresses from SSRT are presented for the same times to rupture. As the times to rupture form SPT and SSRT tests were not the same, the values of stresses for SSRT test were obtained from the regressions fitted to its logarithm trends, as indicated in Figure 15.

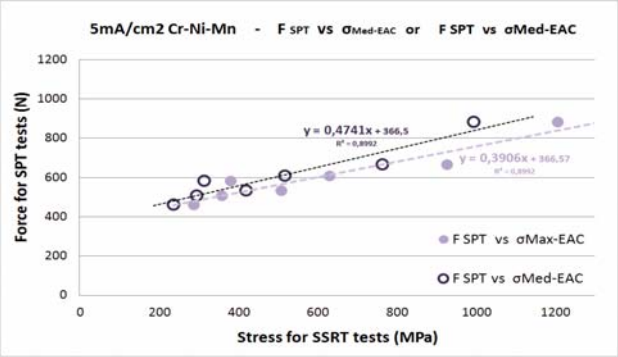

Figure 16. Trends between the force in SPT static load tests and $\sigma_{Med-EAC}$ or $\sigma_{Max-EAC}$, for the same rupture times under the 5mA/cm^2 environment for the Cr-Ni-Mn.

In these circumstances, it should be pointed that the values obtained for the correlation coefficients were K_{Med}=0.47 and K_{Max}=0.39. These results, especially in the case of the mean stress, are not far from those obtained in some creep recent publication using the same sample geometry [16] for the force-stress correlation parameter. This fact allows to estimate tensional values form SPT tests once the model is calibrated with a few SSRT ones. Considering the properties described above, a methodology widely used in small punch creep scenarios [16] can be proposed as a simple and effective way to correlate the results of SPT and conventional tests in embrittlement situations. It is based on matching the same breaking times in both types of tests when performed under the same environment (temperature in the case of creep and dissolution and imposed current in the case of embrittlement scenarios). These two tests, SPT and SSRT, will be equivalent for a given environment when they have similar breaking times.

A geometric hypothesis proposed by the SPT code of practice [12] and widely accepted for small punch creep tests that should be checked for SPT in the hydrogen embrittlement situations in this work. It establishes that when a uniaxial slow strain rate test and a SPT static load one have similar times to rupture, the numerical value of the deformation rate (uniaxial test) and the punch rate (SPT) that take place during the two tests will also be alike. With a view to verifying this property, in Figure 18, SSRT and SPT tests results from both materials and all the tested conditions are graphed in a deformation rate (s^{-1} for SSRT) or punch rate (mm/s for SPT) versus time to rupture chart.

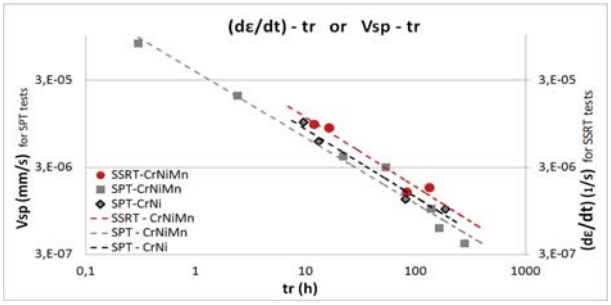

Figure 17. Comparison of punch rate vs rupture time in SPT and deformation rate vs rupture time in SSRT.

As presented in Figure 17, the aforementioned property was satisfied. It can be observed how for the Cr-Ni-Mn steel (squares for SPT and circles for SSRT) the trends plotted denote similar breaking times when the numerical values of the punch rate (SPT) and the deformation rate (SSRT) coincide. In addition, the Cr-Ni SPT results give rise to a trend which is very close to that given by the SPT results of the Cr-Ni-Mn steel, and it is also similar to the trend described by the SSRT on the Cr-Ni-Mn. This last fact indicates that this geometric property works for SPT in embrittlement scenarios, and can be used to predict rupture time by means of SPT. Finally, Figure 18 the load applied versus the punch rate (SPT), or the maximum stress versus the deformation rate (SSRT), were plotted for tests performed on the same material and environment in both cases (Cr-Ni-Mn steel and 5mA/cm^2). Also the results of the SSRT tests under 1mA/cm^2 are plotted in order to show the effect of the aggressiveness of the environment on a given material.

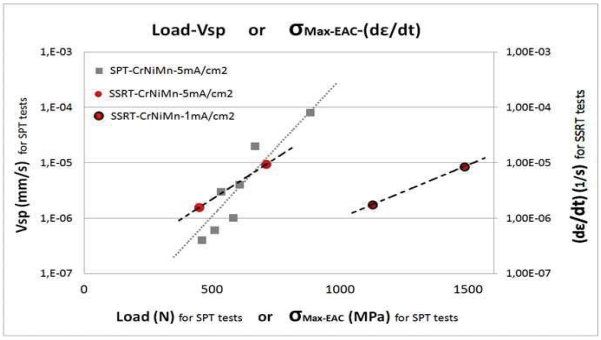

Figure 18. Comparison of punch rate vs load (SPT) and deformation rate vs maximum stress (SSRT) trends for the Cr-Ni-Mn steel.

It seems that, when a SSRT and a SPT test are performed in the same environment, if the maximum stress (SSRT) and the load (SPT) are numerically similar, the deformation rate (SSRT) and the punch rate (SPT) are related by a coefficient Kσ. This property is very useful in order to estimate deformation rates simply by performing a series of SPT tests in a specific environment once its calibrated by reduce set of SSRT tests (determine regression coefficient Kσ). This can be written in a more general way as follows:

$$\frac{d\varepsilon/dt}{V_{sp}} \approx K_\sigma \quad \leftrightarrow \quad F_{SPT} \approx \sigma_{Max-EAC} \tag{3}$$

6. CONCLUSIONS AND FUTURE WORK

In this paper, the Small Punch Test has been re-validated as a method for characterizing materials in embrittlement scenarios.

In a first step, the small punch test was proposed as a simple and economic alternative when it is not possible to perform standard tests in adverse environmental situations. Subsequently, it was proposed for this aim to use SPT under static load tests with the specimen pre-charged and submerged in the environment during the whole test. Also some other result processing techniques widely used in standard stress corrosion cracking tests, and both conventional creep and small punch creep tests, were shown to be adequate.

Based on the experimental results it was proved that:

- The small punch curve under static load in embrittlement environments has the same shape as the one that takes place during both conventional and small punch creep tests, having three zones. The first zone governs the indentation and settlement of the load, the second steady state zone governs the crack propagation and has a quasi-constant punch rate and the third zone governs the final stability and rupture of the specimen.
- It was observed that when a uniaxial slow strain rate test and a SPT static load one have similar maximum stress and load respectively, the numerical value of the deformation rate (uniaxial test) and the punch rate (SPT) that take place during the two tests will be related. Based on this, a simple method is proposed for obtaining equivalent values of deformation rate for given maximum stresses.
- A geometric property was proved, as stated by the code of good practice and as is widely used for small punch creep tests, which establishes that when a uniaxial slow strain rate test and a SPT static load one have similar times to rupture, the numerical value of the deformation rate (uniaxial test) and the punch rate (SPT) that take place during the two tests will also be alike. This is a promising tool to obtain a reference value the threshold stress σ_{EAC} by means of SPT.

The next step in this line of research will be the estimation of stresses from the applied loads could be completed by empirical correlations from the bibliography.

ACKNOWLEDGEMENT

The authors of this paper would like to thank the Spanish Ministry of Economy and Competitivity for the support received for the development of the research projects MAT2011-28796, and MAT2014-58738.

REFERENCES

[1] C. RENAUDIN, "*Utilisation des aciers HLE en conditions de protection cathodique*", Memoire, Conservatoire national des arts et metiers, 1994.
[2] TAO BAI, PENG CHEN, KAISHU GUAN, "Evaluation of stress corrossion cracking susceptibility of sainless steel 304L with surface nanocrystalization by small punch test", Material Science & Engineering A, 561 (2013) 498-506.
[3] ARROYO B., ÁLVAREZ J.A., LACALLE R., GUTIÉRREZ-SOLANA F., GARCÍA T.E., "Environmental effects on R5 steel under cathodic protection and cathodic charge. characterization using the Small Punch Test", Proceedings of the 2nd SSTT, Austria, 2014.
[4] GARCÍA T.E., RODRÍGUEZ C., BELZUNCE F.J., PEÑUELAS I., ARROYO B., "Development of a methodology to study the hydrogen embrittlement of steels by means of the small punch test", Materials Science & Engineering A, 626 (2015), 342-351.
[5] GARCÍA T.E., RODRÍGUEZ C., BELZUNCE F.J., CUESTA I.I., "Effect of hydrogen embrittlement on the tensile properties of CrMoV steels by means of the small punch test", Materials Science & Engineering A, 664 (2016), 165-176.
[6] ARROYO B., ÁLVAREZ J.A., LACALLE R., "Study of the energy for embrittlement damage initiation by SPT means. Estimation of K_{EAC} in aggressive environments and rate considerations", Theorethical and Applied Fracture Mechanics, 86 (2016), 61-68.
[7] GARCÍA T.E., ARROYO B., RODRÍGUEZ C., BELZUNCE F.J., ÁLVAREZ J.A., "Small punch test methodologies for the analysis of the hydrogen embrittlement of structural steels", Theorethical and Applied Fracture Mechanics, 86 (2016), 89-100.
[8] HAMILTON, J.M., "The challenges of Deep-Water Artic Development", International Journal of Offshore and Polar Engineering, 21 (4), (2011), 241-247.
[9] ÁLVAREZ J.A., " *Fisuración inducida por hidrógeno de aceros soldables microaleados. Caracterización y modelo de comportamiento* ", Doctoral Thesis, University of Cantabria, 1998.
[10] LACALLE, R., " *Determinación de las propiedades en tracción y fractura de materiales metálicos mediante ensayos Small Punch* ". Doctoral Thesis, University of Cantabria, 2012.
[11] CWA 15627:2008. "Small Punch Test for Metallic Materials". European Comittee for Standarization (CEN).
[12] LACALLE R., ÁLVAREZ J.A., GUTIÉRREZ-SOLANA F., "Analysis of key factors for the interpretation of small punch test results", Fatigue and Fracture of Engineering Materials & Structures, 31 (2008) 481-489.
[13] M. ESKNER, R. SANDSTROM, "Mechanical property using the small punch test", Journal of Testing and Evaluation, vol 32, Nº 4, January 1995, pp. 282-289.
[14] LACALLE R., ARROYO B., ÁLVAREZ J.A. & GUTIÉRREZ-SOLANA F. "Aproximación basada en el concepto de CTOD para la determinación de la tenacidad mediante probetas Small Punch" Anales de Mecánica de la Fractura, vol. XXVIII, pp. 749-754, 2011.
[15] DOBES, F. & MILIčKA, K., "Application of creep small punch testing in assessment of creep lifetime", Materials Science & Engineering A, vol. 510-511, pp. 440-443, 2009.
[16] ANDRÉS D., LACALLE R., ÁLVAREZ J.A., "Creep property evaluation of light alloys by means of the small punch test: creep master curves", Materials and Design, 96 (2016) 122-130.
[17] D. FINARELLY, M. ROEDIG, F. CARSUGHI, "Small Punch Tests on Austenitic and Martensitic Steels Irradiated in a Spallation Environment with 530 MeV Protons", Journal of Nuclear Materials 328, 2004, pp. 146-150.
[18] M.L. SAUCEDO-MUÑOZ, T. MATSUSHITA, T. HASHIDA, T. SHOJI, H. TAKAHASHI, "Development of a Multiple Linear Regresion Model to Estimate the Ductile-Brittle Trasition Temperature of Ferritic Low-Alloy Steels Based on the Relationship Between Small Punch an Charpy V-Notch Tests", Journal of Testing and Evaluation, Vol 28, No. 5, September 2000, pp. 352-358.
[19] ISO 7539:2011*; "Corrosion of metals and alloys" - Stress corrosion testing.*
[20] ÁLVAREZ, J.A., GUTIÉRREZ-SOLANA, F. "*An elastic-plastic fracture mechanics based methodology to characterize cracking behavior and its applications to environmental assisted processes*", Nuclear Engineering and Design 188, pp. 185-202, 1998.
[21] CAYÓN, A., ÁLVAREZ, J.A., GUTIÉRREZ-SOLANA, F., DE CARLOS, A., "*Application of new fracture mechanics concepts to hydrogen damage evolution*", Final Report ECSC Contract. No 7210-PE-110, University of Cantabria, 2001.
[22] FAURIE J.P., MONNIER P., NIKU-LARI A., " *Guide du dessinateur: les concentrations de contraintes* ", CETIM, 2000, ISBN-10 2854004949, ISBN-13: 978-2854004946.